

Comparing different light-emitting diodes as light sources for long path differential optical absorption spectroscopy NO₂ and SO₂ measurements

This article has been downloaded from IOPscience. Please scroll down to see the full text article.

2012 Chinese Phys. B 21 119301

(<http://iopscience.iop.org/1674-1056/21/11/119301>)

View [the table of contents for this issue](#), or go to the [journal homepage](#) for more

Download details:

IP Address: 61.190.88.160

The article was downloaded on 11/01/2013 at 04:53

Please note that [terms and conditions apply](#).

Comparing different light-emitting diodes as light sources for long path differential optical absorption spectroscopy NO₂ and SO₂ measurements*

Chan Ka-Lok(陈嘉乐)^{a)b)}, Ling Liu-Yi(凌六一)^{a)}, Andreas Hartl^{b)},
Zheng Ni-Na(郑尼娜)^{a)}, Gerrit Kuhlmann^{b)}, Qin Min(秦敏)^{a)}, Sun You-Wen(孙友文)^{a)},
Xie Pin-Hua(谢品华)^{a)†}, Liu Wen-Qing(刘文清)^{a)}, and Mark Wenig^{b)}

^{a)}Anhui Institute of Optics and Fine Mechanics, Chinese Academy of Sciences, Hefei 230031, China

^{b)}School of Energy and Environment, City University of Hong Kong, Hong Kong, China

(Received 30 March 2012; revised manuscript received 23 May 2012)

In this paper, we present a comparison of different light-emitting diodes (LEDs) as the light source for long path differential optical absorption spectroscopy (LP-DOAS) atmospheric trace gas measurements. In our study, we use a fiberoptic design, where high power LEDs used as the light source are coupled into the telescope using a Y shape fiber bundle. Two blue and one ultraviolet (UV) LEDs with different emission wavelength ranges are tested for NO₂ and SO₂ measurements. The detailed description of the instrumental setup, the NO₂ and SO₂ retrieval procedure, the error analysis, and the preliminary results from the measurements carried out in Science Island, Hefei, Anhui, China are presented. Our first measurement results show that atmospheric NO₂ and SO₂ have strong temporal variations in that area and that the measurement accuracy is strongly dependent on the visibility conditions. The measured NO₂ and SO₂ data are compared to the Ozone Monitoring Instrument (OMI) satellite observations. The results show that the OMI NO₂ product underestimates the ground level NO₂ by 45%, while the OMI SO₂ data are highly influenced by clouds and aerosols, which can lead to large biases in the ground level concentrations. During the experiment, the mixing ratios of the atmospheric NO₂ and SO₂ vary from 8 ppbv to 36 ppbv and from 3 ppbv to 18 ppbv, respectively.

Keywords: light-emitting diode, fiber optic designed telescope, NO₂ measurement, SO₂ measurement

PACS: 93.90.+y

DOI: 10.1088/1674-1056/21/11/119301

1. Introduction

Differential optical absorption spectroscopy (DOAS) is a powerful remote sensing technique used for atmospheric trace gas measurements.^[1] The DOAS allows the quantitative detection of a broad variety of atmospheric trace gases by the distinctive narrow band absorption structures of different trace gases. Active long path differential optical absorption spectroscopy (LP-DOAS) instruments are used to realize long optical paths in the atmosphere from several hundreds of meters to more than 20 km. Such long paths are essential for the detection of atmospheric trace gases with mixing ratios in the ppbv to pptv range by the DOAS.

The conventional LP-DOAS instrumental setup combines the emitting and the receiving telescopes into one single instrument sharing the same main

mirror.^[2,3] Operating such an instrument requires very accurate alignment of the optical components. A 100 μm displacement of the light source, which can easily be caused by mechanical instability and thermal expansion,^[4] may lead to an intensity loss of up to one third of the total light. Moreover, the positions and the sizes of the plane mirrors are critical to the potential efficiency of the setup, since they shade the central part of the main mirror. A fiberoptic designed LP-DOAS telescope avoids the problems of the conventional telescope setup and provides a higher light performance throughput.^[4] This novel telescope design allows the use of weaker light sources like light-emitting diodes (LEDs).

Artificial light sources for the LP-DOAS do not only show a broad-band thermal spectrum defined by Planck's law, but can also have spectral structures

*Project supported by the National High-Technology Research and Development Program of China (Grant No. 2009AA063006) and the National Natural Science Foundation of China (Grant No. 60808034).

†Corresponding author. E-mail: phxie@aiofm.ac.cn

© 2012 Chinese Physical Society and IOP Publishing Ltd

<http://iopscience.iop.org/cpb> <http://cpb.iphy.ac.cn>

similar to those of the trace gas absorption. In particular xenon arc lamps, which are most commonly used in active DOAS measurements, show characteristic emission lines that change both in intensity and spectral shape during the lamp lifetime. The wide spectral emission range of the xenon arc lamps is also known to cause the stray light problem in the spectrometer.^[5] LEDs offer alternate options for the light sources in the active DOAS measurements. Compared to xenon arc lamps, modern LEDs have high power efficiencies and longer lifetimes, some of them even give higher intensities in the emitting spectral range. However, some LEDs show characteristic structures like the Etalon effect, which is known to interfere with the trace gas absorption structures.^[5,6] Long term DOAS measurements of NO₂ using an LED as the light source have already been demonstrated by Chan *et al.*,^[7] some cavity enhanced DOAS instruments^[8] also used the LED as the light source.^[9–11] However, the ultraviolet (UV) LEDs for atmospheric trace gas measurements are still under investigation.

Nitrogen dioxide (NO₂) is an atmospheric pollutant, which plays an important role in both tropospheric and stratospheric chemistry. NO₂ is an important ozone (O₃) precursor in the troposphere, while being a catalyst for O₃ destruction in the stratosphere.^[12] Solomon *et al.*^[13] found that NO₂ also significantly contributed in radiatively heating the earth's atmosphere. NO₂ causes acid rain, which is known to have adverse effects on soil, forest, and water resources. Moreover, NO₂ in high concentration is harmful to humans. Atmospheric NO₂ is mainly produced by anthropogenic processes. About 50% of the global NO₂ emission is contributed by fossil fuel combustion.^[14] Sulphur dioxide (SO₂) is an atmospheric pollutant emitted from both natural and anthropogenic sources, which leads to aerosol formation and acid deposition in the atmosphere. SO₂ in high concentration can have adverse effects on human health. Anthropogenic SO₂ emission in China contributed about 25% of global emissions and more than 90% of East Asian emissions since the 1990s.^[15–19] The total SO₂ emission was increased by about 53% from 2000 to 2006.^[20] Power plant emissions are the major sources of SO₂ in China.^[20] The concentrations of atmospheric NO₂ and SO₂ usually vary rapidly in most urban areas, hence it is necessary to measure NO₂ and SO₂ concentrations with a high temporal resolution for air quality management and control.

The application of LEDs as a light source and the

new fiberoptic designed telescope are both relatively new techniques for DOAS measurements, and here we combine both techniques together to perform atmospheric NO₂ and SO₂ measurements. In this paper, we present the experimental setup and the first atmospheric NO₂ and SO₂ measurement results of the LED based fiberoptic design LP-DOAS instrument in Hefei. Two different blue LEDs and one UV LED were tested for NO₂ and SO₂ measurements respectively. A detailed description of the instrument setup, the data retrieval procedure, and the error analysis are presented.

The experiment was conducted on Science Island, Hefei, Anhui, China, a remote site about 12 km southwest of the city center hosting a number of research facilities belonging to the Chinese Academy of Sciences and few residential buildings. The telescope and the retro reflector were located on the sixth floor of two buildings separated by a distance of 340 m, and were about 20 m above ground level, resulting in a total absorption path of 680 m. The measurement path crossed the main road of the island.

2. Differential optical absorption spectroscopy

The classical absorption spectroscopy describes the loss of intensity of the light passing through a volume of absorbing matter by the Lambert–Beer law. For atmospheric radiative transfer, it takes the form

$$I(\lambda) = I_0(\lambda) \exp \left(-L \sum_i \sigma_i(\lambda) c_i + \epsilon_M + \epsilon_R \right), \quad (1)$$

where I represents the light intensity of the light beam after passing through an atmospheric layer of thickness L , I_0 represents the initial light intensity of the light beam emitted by the light source, σ_i denotes the absorption cross section of trace gas i , and c_i is its mean concentration along the light path. The ϵ_M and ϵ_R denote the Mie and the Rayleigh extinction coefficients, respectively. In practice, equation (1) cannot be used for trace gas measurements, if the initial intensity or the other extinction processes cannot be quantified precisely.

To overcome this problem, the DOAS^[1] separates the narrow band trace gas absorptions from the broad band parts that are caused mainly by broad band absorption and atmospheric scattering. The narrow

band absorptions are then used for the quantitative detection of the different trace gases

$$\sigma(\lambda) = \sigma_b(\lambda) + \sigma'(\lambda), \quad (2)$$

where σ_b represents the broad band scattering and absorption, while σ' represents the narrow band absorption structures of the individual trace gases, which vary rapidly with wavelength λ . The trace gas analysis then focuses on the differential absorption structures, and the Lambert–Beer law can be written as

$$\begin{aligned} I(\lambda) &= I_0(\lambda) \exp\left(-L \sum_i \sigma'_i(\lambda) c_i\right) A(\lambda) \\ &= I'_0(\lambda) \exp\left(-L \sum_i \sigma'_i(\lambda) c_i\right), \end{aligned} \quad (3)$$

where A summarizes all the broad-band effects, including the instrument effect, the Mie and the Rayleigh scatterings, and the broad-band absorptions of the trace gases, and I'_0 represents the intensity without the differential absorption component. Thus, the differential optical density D' can be defined as the logarithm of the ratio of I'_0 to I

$$D' = \ln\left(\frac{I'_0(\lambda)}{I(\lambda)}\right) = L \sum_i \sigma'_i(\lambda) c_i. \quad (4)$$

The broad-band structures from the absorptions and the scatterings are removed by dividing the spectrum by a fit polynomial of appropriate degree and/or applying a high-pass filter, which further removes the broad-band structures.^[21]

3. Experimental setup

Figure 1 shows the schematic diagram of the LED based fiber optic design LP-DOAS instrument. A blue/UV LED is used as the light source, a telescope with 220 mm diameter and 650 mm focal length acts as the transmitting and receiving component, and an array of retro reflectors are placed at the other side of the measurement path. This setup is very similar to the ones described in Refs. [4] and [7]. Six transmitting fibers and one receiving fiber all 200 μm in diameter and 0.22 in numerical aperture are connected in a 4 m Y shape bundle directing light from the LED into the telescope and from the telescope into the spectrometer. A quartz glass lens with a focal length of 17.5 mm is used to couple the light from the LED to the transmitting fibers. The combined end of the Y shape fiber bundle is placed near

the focal point of the main mirror of the telescope. The light reflected back by the retro reflector array is collected by the same telescope and redirected to the spectrograph by the receiving fiber for spectral analysis. As the strongest differential absorption structures of NO_2 and SO_2 locate at different wavelength regions, two different spectrometers are used for NO_2 and SO_2 measurements. In this study, an Ocean Optic Maya 2000 Pro spectrometer with a Hamamatsu S10420 charge-coupled device (CCD) detector was used for the NO_2 measurements. The spectral resolution of this spectrometer was 0.291 nm in the wavelength range from 368.10 nm to 582.62 nm. For the SO_2 measurements, an Ocean Optic QE65000 spectrometer with a Hamamatsu S7031-1006 CCD detector was used. The spectral wavelength range was from 249.78 nm to 369.24 nm with a spectral resolution of 0.726 nm.

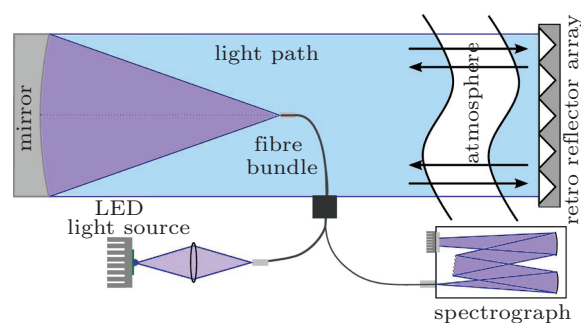


Fig. 1. (colour online) Setup of the LED based fiber optic design fiber LP-DOAS instrument.

The wavelength calibration of the spectrometer was carried out by using the emission lines of a Mercury lamp, and the recorded emission line of the Mercury lamp within the fitting wavelength region was treated as the instrument function of the spectrometer. In order to obtain the literature reference spectra with the instrument resolution, the high resolution literature reference spectra were convolved with the instrument function.

In this study, three setups with different blue and UV LEDs were used for atmospheric NO_2 and SO_2 measurements. Setup 1 used a CREE XR-E 7090 blue LED (455–485 nm, FWHM) as the light source and was installed from 26 October 2011 15:00 to 27 October 2011 07:00 (local time), setup 2 used a CREE XP-E 7090 royal blue LED (435–465 nm, FWHM) as the light source and was installed from 19 November 2011 15:00 to 21 November 2011 09:00 (local time). Both setups 1 and 2 were used for NO_2 measurements. During the experiment, the currents of both

blue LEDs were set at 500 mA, resulting in approximately 500 mW optical output power. Setup 3 used a UV TOP 280 FW UV LED (270–290 nm, FWHM) as the light source for SO₂ measurement and was installed from 06 January 2012 11:00 to 08 January 2012 16:00 (local time). During the experiment, the current of the UV LED was set at 20 mA, resulting in approximately 800 μW optical output power. The emission spectra of those LEDs are shown in Fig. 2. All setups used the same telescope, fiber bundle, and retro reflectors, and measured along the same measurement path.

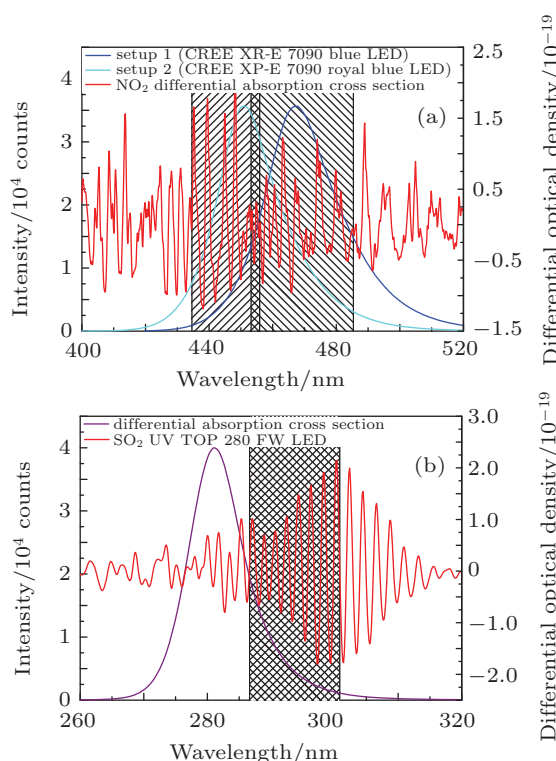


Fig. 2. (colour online) Emission spectra of the LEDs used in the experiment. (a) The blue curve shows the emission spectrum of the CREE XR-E 7090 blue LED used in setup 1, the cyan curve shows the emission spectrum of the CREE XP-E 7090 royal blue LED used in setup 2. Both LEDs are used for NO₂ measurements. The red curves show the differential absorption cross section of NO₂. The hatched regions indicate the DOAS fitting range for setups 1 and 2. (b) The violet curve shows the emission spectrum of the UV TOP 280 FW UV LED used for SO₂ measurements in setup 3. The red curve shows the differential absorption cross section of SO₂. The hatched regions indicate the DOAS fitting range.

4. Retrieval procedure

The recorded spectra are analyzed using the DOAS retrieval software DOASIS.^[22] All measurement spectra are corrected for offset and dark cur-

rents before dividing by the spectrum of the LED. Subsequently, the logarithm is taken. A high pass filter is applied to the spectrum by subtracting a binomial smoothing filter in the order of 1000 to eliminate the broad-band effects in the spectrum. In order to remove the remaining broad-band effects in the spectrum, a fifth-order polynomial is included in the DOAS fitting procedure. Five trace gases are included in the DOAS fit for NO₂ measurements: NO₂,^[23] H₂O,^[24] glyoxal (CHOCHO),^[25] O₃,^[26] and O₄.^[27] Three trace gases are included in the DOAS fit for SO₂ measurements: SO₂,^[28] O₃,^[26] and HCHO.^[29] In order to correct for small uncertainties, the squeeze and shift of the literature reference spectra are allowed during the wavelength mapping procedure. The trace gas mixing ratios are retrieved by dividing the retrieved slant column densities by the measurement path length and the air density.

5. Results

5.1. NO₂ measurements

Two blue LEDs with different emission wavelength ranges were used for NO₂ measurements. The spectral fitting ranges for setups 1 and 2 were from 453.2 nm to 485.4 nm and from 434.6 nm to 455.9 nm, respectively (see Fig. 2(a)). Figure 3 shows the DOAS fit example of a spectrum measured with setup 1 on 26 October 2011 at 15:04 (local time) with a slant column density of NO₂ of $(2.48 \pm 0.17) \times 10^{16} \text{ cm}^{-2}$ corresponding to (14.3 ± 1.0) ppbv in the volume mixing ratio. Figure 4 shows the DOAS fit example of a spectrum measured with setup 2 on 19 November 2011 at 15:12 (local time) with NO₂ slant column density of $(1.46 \pm 0.07) \times 10^{16} \text{ cm}^{-2}$ corresponding to (8.4 ± 0.4) ppbv in the volume mixing ratio. The measurement error is estimated using the residuum of the fit.^[21] The temporal resolutions of the two setups are different because of the different visibility conditions. Setup 1 measured an atmospheric spectrum with an exposure time of 50 ms and 3000 scans, resulting in a temporal resolution of 2.5 min, while setup 2 measured an exposure time of 10 ms and 6000 scans, resulting in a temporal resolution of 1 min. Both setups were measured at a different time with different atmospheric conditions, therefore, a detailed error analysis is presented to analyse the discrepancy between the two setups.

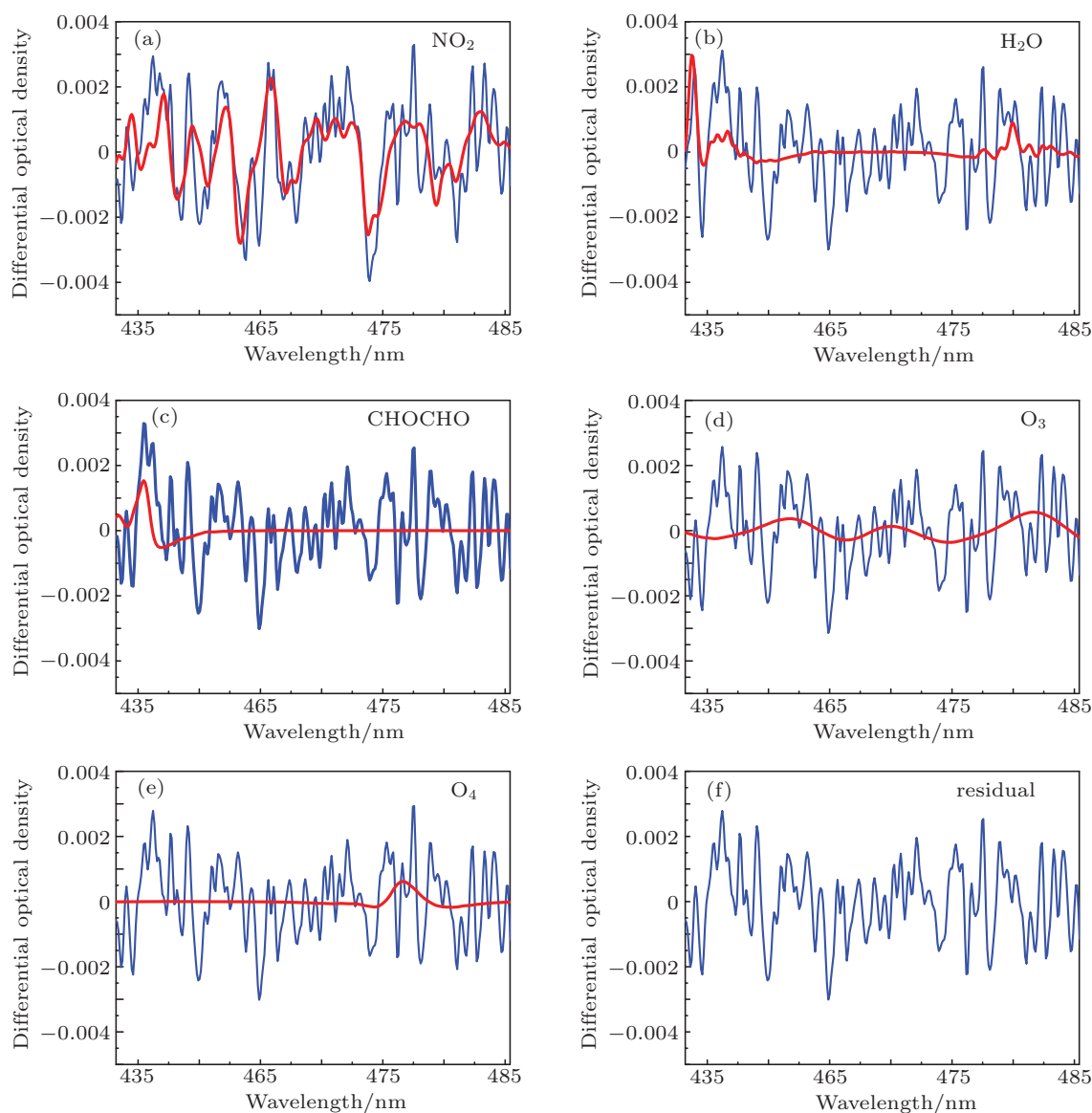


Fig. 3. (colour online) The DOAS fit from a spectrum taken on 26 October 2011 at 15:04 (local time) with $(2.48 \pm 0.17) \times 10^{16} \text{ cm}^{-2}$ NO_2 slant column density corresponding to (14.3 ± 1.0) ppbv in the volume mixing ratio. The differential absorption cross sections (red curves) and the sum of the fit residual and the differential absorption cross sections (blue curves) of (a) NO_2 , (b) H_2O , (c) CHOCHO , (d) O_3 , and (e) O_4 are shown. Panel (f) shows the residual.

Two LEDs were tested for NO_2 measurements on 26 October 2011 and 19 November 2011 respectively. The time series of the measured atmospheric NO_2 mixing ratios of setups 1 and 2 are shown in Fig. 5. Due to the different visibility conditions, the temporal resolutions of the two setups are slightly different. The temporal resolutions of setups 1 and 2 are 2.5 min and 1 min, respectively. The NO_2 measurement results from both setups show strong temporal variations with maximum values in the evening. The maxima of NO_2 in the morning and evening rush hours

are commonly observed in cities. During the day, NO_2 is photolytically destroyed. The mean NO_2 mixing ratio over the entire measurement period of setup 1 is 22.3 ppbv, and the mean error of the measurements is 1.5 ppbv. The maximum and the minimum mixing ratios of NO_2 recorded with setup 1 are 35.7 ppbv and 11.0 ppbv, respectively. The mean NO_2 mixing ratio over the entire measurement period of setup 2 is 16.5 ppbv with a mean error of 0.7 ppbv. The maximum and the minimum mixing ratios of NO_2 recorded with setup 2 are 25.9 ppbv and 7.9 ppbv, respectively.

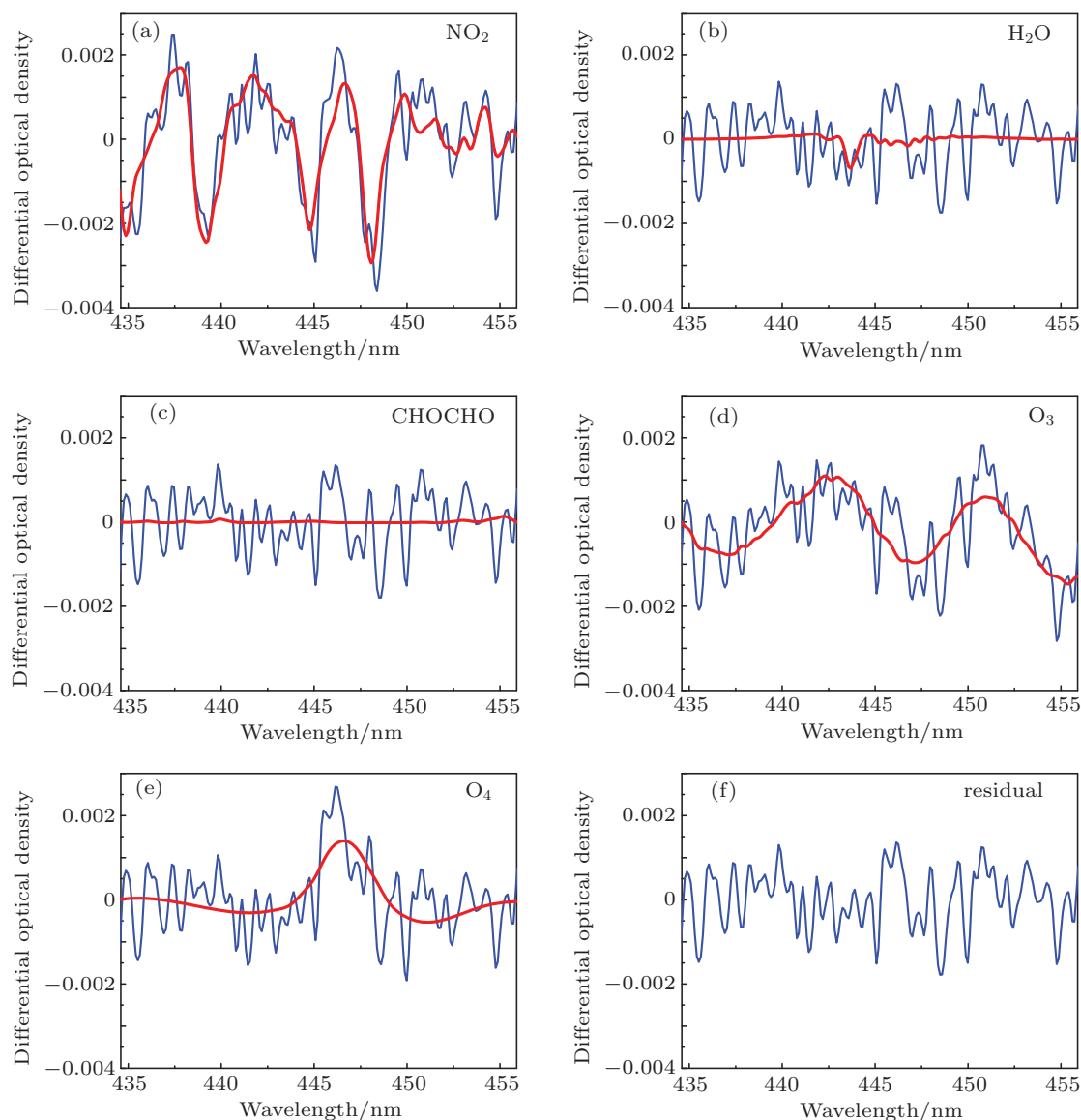


Fig. 4. (colour online) The DOAS fit from a spectrum taken on 19 November 2011 at 15:12 (local time) with $(1.46 \pm 0.07) \times 10^{16} \text{ cm}^{-2}$ NO_2 slant column density corresponding to (8.4 ± 0.4) ppbv in the volume mixing ratio. The differential absorption cross sections (red curves) and the sum of the fit residual and the differential absorption cross sections (blue curves) of (a) NO_2 , (b) H_2O , (c) CHOCHO , (d) O_3 , and (e) O_4 are shown. Panel (f) shows the residual.

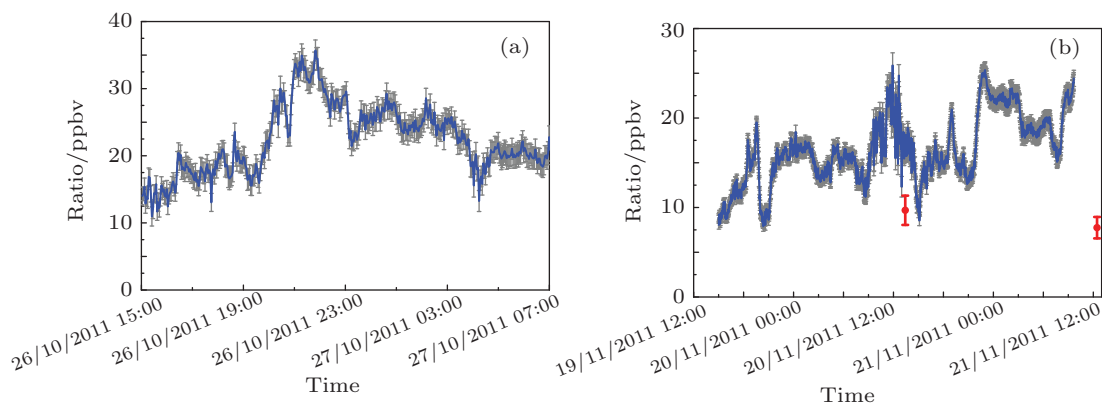


Fig. 5. (colour online) (a) Mixing ratio of atmospheric NO_2 measured using the fiber LP-DOAS with the CREE XR-E 7090 blue LED as the light source (setup 1) from 26 October 2011 15:00 to 27 October 2011 07:00 (local time). (b) The blue curve shows the mixing ratio of atmospheric NO_2 measured using the fiber LP-DOAS with the CREE XP-E 7090 royal blue LED as the light source (setup 2) from 19 November 2011 15:00 to 21 November 2011 09:00 (local time), while the red dots indicate the OMI measurement values.

A further error analysis of the LP-DOAS measurements is done by comparing the estimated errors derived from the DOAS fit to the one gained from analyzing the high frequency variation of the measured time series. The high frequency variation in the time series is assumed to be dominated by the instrument noise, as the concentration of the trace gases integrated through a long measuring path should vary on a larger time scale. A high pass filter is applied to the time series by subtracting a low pass smoothing filter with a window of an hour. The results show that the 1σ standard deviations of the high frequency variation of the time series of setups 1 and 2 are 1.5 ppbv and 0.9 ppbv, respectively. The results agree well with the mean estimated errors of the time series, which are 1.5 ppbv and 0.7 ppbv for setups 1 and 2, respectively. In order to estimate the effect of the stray light on the measurement accuracy, we compare day and night time data. The results show that the mean measurement error of the night time data is about 33% smaller than that of the day time data, so the stray light seems to contribute about one third of the total error.

The measurement error of setup 1 is about 2.14 times higher than that of setup 2. There are mainly two reasons. Firstly, the visibility is lower during the measurement period of setup 1; secondly, the differential absorption structures of NO_2 in the wavelength range of the LED of setup 1 are weaker than those of setup 2. According to the received light intensity, the visibility during the measurement period of setup 2 is about 5 times better than that of setup 1, since both setups are set to the same initial intensity. In order to achieve the same exposure, the integration time of setup 1 has to be 5 times longer than that of setup 2, hence the temporal resolution is 5 times lower. However, we only increased the integration time of setup 1 by a factor of 2.5 in order to achieve a certain time resolution. Using the standard error propagation analysis, we find that this effect leads to about 40% larger errors in setup 1. The strength of the trace gas absorption in the wavelength range also affects the signal-to-noise ratio and the error, as well as the detection limit. The differential absorption structures of NO_2 in the fitting wavelength range of setup 2 are about 80% stronger than those in setup 1 (see Fig. 2), and the error caused by this effect in setup 1 is estimated to be about 80% larger than that in setup 2. Thus, choosing a LED with a suitable emission wavelength range is very important. These two effects explain about 95% of the discrepancy, the remaining discrep-

ancy may result from different stray light conditions and temperature instabilities of the spectrograph.

We compare the LP-DOAS NO_2 measurements to the Ozone Monitoring Instrument (OMI) satellite NO_2 observations. In this study, NASA's OMI tropospheric NO_2 data product is used.^[30] The tropospheric NO_2 vertical column density measured by the OMI is converted to the ground level concentration by using the a-priori NO_2 profile used in the OMI retrieval. The OMI NO_2 data are shown in Fig. 5(b). Generally, higher NO_2 levels can be observed over cities. The measurement site is located on the edge of the main NO_2 plume from the city. During the measuring period, there is only one coinciding OMI NO_2 measurement with LP-DOAS setup 2. The error bars of the LP-DOAS and the OMI measurements do not overlap with each other, which indicates that the NO_2 measurements of OMI are significantly lower than the LP-DOAS measurements. The comparison result shows that the OMI measurement is about 45% lower than the LP-DOAS measurement result, which indicates that the OMI satellite underestimates the ground NO_2 level. This observation agrees with a similar study in Hong Kong.^[7]

5.2. SO_2 measurements

Atmospheric SO_2 measurements were performed using a UV LED with an emission wavelength range from 270 nm to 290 nm (FWHM) as the light source. The spectral fitting range for the SO_2 measurements was from 286.6 nm to 300.9 nm (see Fig. 2(b)). Figure 6 shows the DOAS fit example of a spectrum measured by setup 3 on 06 January 2012 at 13:28 (local time) with a slant column density of SO_2 of $(2.95 \pm 0.12) \times 10^{16} \text{ cm}^{-2}$ corresponding to (17.4 ± 0.7) ppbv in volume mixing ratio. The measurement error is estimated using the same method as that in the NO_2 measurements. Since the intensity of the UV LED was much lower than that of the blue LED and the measurements were very sensitive to the visibility condition, we adapted a slightly different procedure for the SO_2 measurements. For the SO_2 measurements, we measured an atmospheric spectrum with a maximum of 10 scans. One scan was a spectrum with a peak intensity about two thirds of the saturation of the detector, and typically took 40 s to 60 s depending on the visibility. In order to achieve a certain temporal resolution, the total sampling time for 1 measurement (10 scans) was limited to 10 min, if a longer exposure was required, the number of scans was reduced.

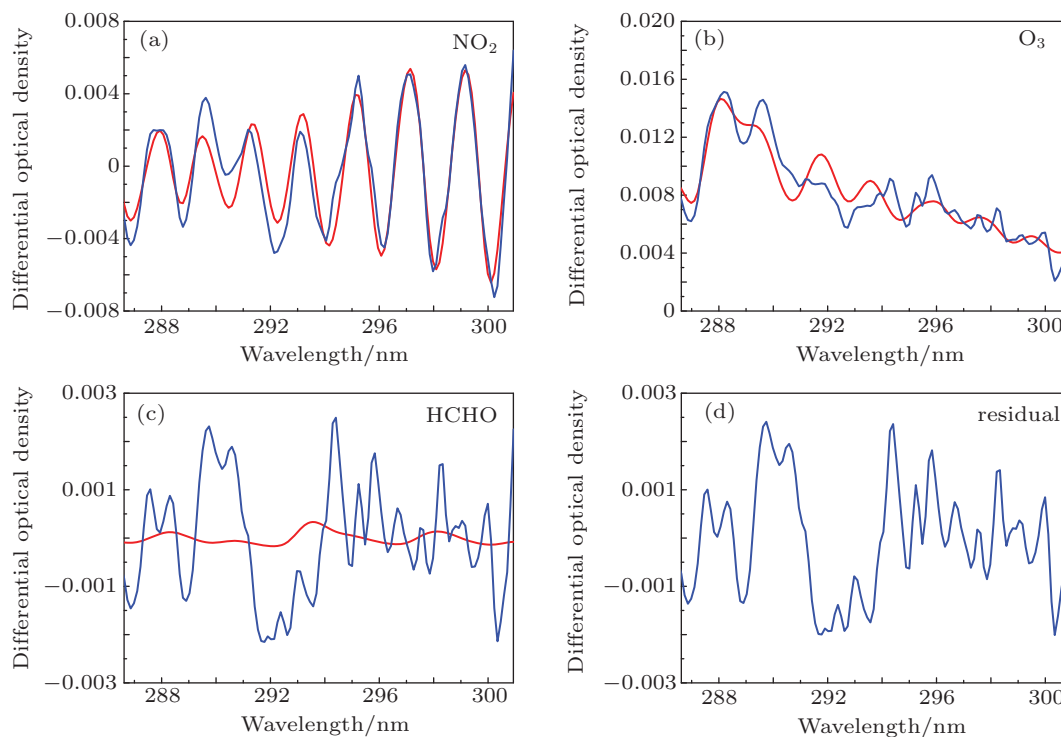


Fig. 6. (colour online) The DOAS fit from a spectrum taken on 06 January 2012 at 13:28 (local time) with $(2.95 \pm 0.12) \times 10^{16} \text{ cm}^{-2}$ SO_2 slant column density corresponding to (17.4 ± 0.7) ppbv in the volume mixing ratio. The differential absorption cross sections (red curves) and the sum of the fit residual and the differential absorption cross sections (blue curves) of (a) SO_2 , (b) O_3 , and (c) HCHO are shown. Panel (d) shows the residual.

The UV LED was tested for SO_2 measurements on the island from 06 January 2012 11:00 to 08 January 2012 16:00 (local time). The time series of the measured atmospheric SO_2 mixing ratios are shown in Fig. 7. During the measuring period, strong haze and fog arose at night, worsening the visibility conditions. Hence, the system could not measure at night. The temporal resolution of the SO_2 measurements is about 10 min depending on the visibility conditions. The SO_2 measurement results show strong temporal variations with peak values at noon. The mean SO_2 mixing ratio over the entire measurement period is 8.4 ppbv, and the mean error of the measurements is 0.9 ppbv. The maximum and the minimum SO_2 mixing ratios recorded by the system are 17.4 ppbv and 2.5 ppbv, respectively. A further error analysis is done by using the same method as that in the NO_2 measurements. The 1σ standard deviation of the high frequency variation of the SO_2 time series is 0.80 ppbv, which also agrees well with the mean estimated error derived from the DOAS analysis. Due to the bad weather at night during the measurement period, the estimation of the error caused by stray light is not possible.

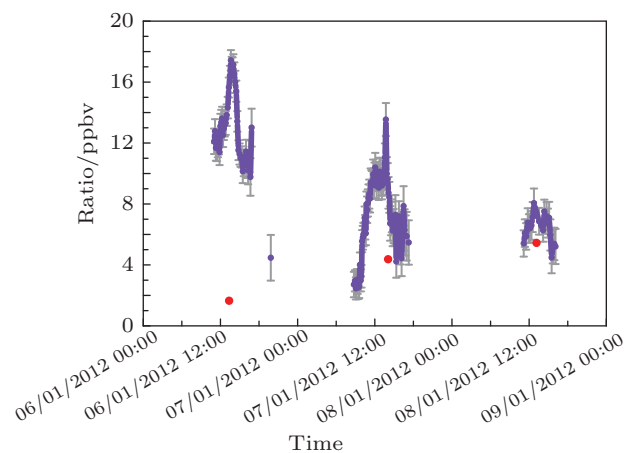


Fig. 7. (colour online) Mixing ratio of atmospheric SO_2 measured using the LED fiber LP-DOAS with the UV TOP 280 FW ultraviolet LED as the light source (setup 3) from 06 January 2012 11:00 to 08 January 2012 16:00 (local time). Error bars of the OMI measurements are not shown, since they are not included in the OMI SO_2 product. OMI data on 7 and 8 of January 2012 are cloud contaminated with cloud fractions of 0.30 and 0.37, respectively.

We compare the LP-DOAS SO_2 measurements with NASA's OMI SO_2 data product.^[31] The air mass factors used for the retrieval are corrected for ground albedo and stratospheric ozone.^[32] The SO_2 vertical

column density measured by the OMI is converted to the ground level concentration by assuming that SO₂ is evenly distributed within a 3 km height planetary boundary layer.^[31] The SO₂ OMI data are shown in Fig. 7. Error bars of the OMI data are not provided here, since they are not included in the OMI data product. Generally, the OMI observations show higher SO₂ values over cities, the SO₂ values over Hefei are relatively low compared to those of other cities nearby. The comparison results show that the LP-DOAS SO₂ measurements do not agree well with the OMI observations. In general, the OMI gives SO₂ values 66% lower than those obtained by the LP-DOAS. The OMI SO₂ data product has been reported to have quite large random errors,^[32] the error of annually averaged SO₂ vertical column density over polluted regions is about 45%–80%.^[33] The SO₂ measurement accuracy of the OMI is highly influenced by clouds and aerosols, which can lead to a large bias in the ground level concentrations.

6. Conclusions

In this paper, we described the experimental setup, the data retrieval procedure and an error analysis of the LED based fiberoptics LP-DOAS for both NO₂ and SO₂ measurements. Atmospheric measurements of NO₂ and SO₂ were performed in Hefei, Anhui, China with a total absorption path of 680 m at about 20 m above ground level. The system used high power LEDs as the light source to measure NO₂ and SO₂ absorptions in the atmosphere. Two blue LEDs and one UV LED with different emission wavelength ranges were tested for NO₂ and SO₂ measurements, respectively. The measurement results showed that the atmospheric NO₂ and SO₂ had strong variations. The measurement accuracy was strongly dependent on the visibility. The stray light was estimated to contribute about 33% to the total measurement errors for the NO₂ measurements. The comparison of the LP-DOAS measurements with the OMI satellite observations showed that the OMI NO₂ product underestimated the ground level NO₂ by 45% when using the a-priori profile from the OMI retrieval for the conversion of vertical column densities to ground concentrations. The OMI SO₂ data are highly influenced by clouds and aerosols, which can lead to a large bias in the ground level concentrations. During the experiment, the mixing ratio of atmospheric NO₂ varied from 8 ppbv to 36 ppbv. The mean mixing ratios of

NO₂ over the entire measurement period of the two setups were 22.3 ppbv and 14.1 ppbv, respectively. The mixing ratio of atmospheric SO₂ varied from 3 ppbv to 18 ppbv during the entire measuring period. The mean mixing ratio of SO₂ during the experiment was 8.4 ppbv. Our first results showed that the LED fiber LP-DOAS is feasible and suitable for monitoring NO₂ and SO₂ in the ambient air.

References

- [1] Platt U, Perner D and Patz H 1979 *J. Geophys. Res.* **84** 6329
- [2] Axelsson H, Galle B, Gustavsson K, Ragnarsson P and Rudi M 1990 *Dig. Top. Meet. Opt. Remote Sens. Atmos. OSA* **4** 641
- [3] Qin M, Xie P, Liu J, Liu W and Wei Q 2005 *Spectroscopy and Spectral Analysis* **8** 1463
- [4] Merten A, Tschirter J and Platt U 2011 *Appl. Opt.* **50** 783
- [5] Kern C, Trick S, Rippel B and Platt U 2006 *Appl. Opt.* **45** 2077
- [6] Sihler H, Kern C, Pöhler D and Platt U 2009 *Opt. Lett.* **34** 3716
- [7] Chan K L, Pöhler D, Kuhlmann G, Hartl A, Platt U and Wenig M O 2012 *Atmospheric Measurement Techniques* **5** 901
- [8] Platt U, Meinen J, Pöhler D and Leisner T 2009 *Atmospheric Measurement Techniques* **2** 713
- [9] Langridge J M, Ball S M and Jones R L 2006 *Analyst* **131**
- [10] Meinen J, Thieser J, Platt U and Leisner T 2010 *Atmospheric Chemistry and Physics* **10** 3901
- [11] Thalman R and Volkamer R 2010 *Atmospheric Measurement Techniques* **3** 1797
- [12] Crutzen P 1970 *Quarterly Journal of the Royal Meteorological Society* **96** 320
- [13] Solomon S, Portmann R W, Sanders R W, Daniel J S, Madsen W, Bartram B and Dutton E G 1999 *J. Geophys. Res.* **104** 12047
- [14] Lee D S, Köhler I, Grobler E, Rohrer F, Sausen R, Gallardo-Klenner L, Olivier J G J, Dentener F J and Bouwman A F 1997 *Atmospheric Environment* **31** 1735
- [15] Streets D G, Tsai N Y, Akimoto H and Oka K 2000 *Atmospheric Environment* **34** 4413
- [16] Streets D G, Wu Y and Chin M 2006 *Geophysical Research Letters* **33** L15806
- [17] Streets D G, Yu C, Wu Y, Chin M, Zhao Z, Hayasaka T and Shi G 2008 *Atmospheric Research* **88** 174
- [18] Streets D G, Yan F, Chin M, Diehl T, Mahowald N, Schultz M, Wild M, Wu Y and Yu C 2009 *J. Geophys. Res.* **114** D00d18
- [19] Ohara T, Akimoto H, Kurokawa J, Horii N, Yamaji K, Yan X and Hayasaka T 2007 *Atmospheric Chemistry and Physics* **7** 4419
- [20] Lu Z, Streets D G, Zhang Q, Wang S, Carmichael G R, Cheng Y F, Wei C, Chin M, Diehl T and Tan Q 2010 *Atmospheric Chemistry and Physics* **10** 6311
- [21] Stutz J and Platt U 1996 *Appl. Opt.* **35** 6041
- [22] Kraus S 2005 *DOASIS A Framework Design for DOAS* (Ph.D. thesis) (Mannheim: University of Mannheim)

- [23] Voigt S, Orphal J and Burrows J P 2002 *J. Photochem. Photobiol.* **149** 1
- [24] Rothmann L, Barbe A, Benner D C, Brown L, Camy-Peyret C, Carleer M, Chance K, Clerbaux C, Dana V, Devi V, Fayt A, Flaud J M, Gamache R, Goldman A, Jacquemart D, Jucks K, Lafferty W, Mandin J Y, Massie S, Nemtchinov V, Newnham D, Perrin A, Rinsland C, Schroeder J, Smith K, Smith, M, Tang K, Toth R, Auwera J V, Varanasi P and Yoshino K 2003 *J. Quant. Spectrosc. Radiat. Transfer* **82** 5
- [25] Volkamer R, Spietz P, Burrows J and Platt U 2005 *J. Photochem. Photobiol.* **172** 35
- [26] Voigt S, Orphal J, Bogumil K and Burrows J P 2001 *J. Photochem. Photobiol.* **143** 1
- [27] Greenblatt G, Orlando J, Burkholder J and Ravishankara A 1990 *J. Geophys. Res.* **95** 18577
- [28] Vandaele A, Simon P, Guilmot M, Carleer M and Colin R 1994 *J. Geophys. Res.* **99** 25599
- [29] Meller R and Moortgat G K 2000 *J. Geophys. Res.* **105** 7089
- [30] Bucsela E, Celarier E, Wenig M, Gleason J, Veefkind P, Boersma K and Brinksma E 20006 *IEEE Transactions on Geoscience and Remote Sensing* **44** 1245
- [31] Krotkov N, Carn S, Krueger A, Bhartia P and Yang K 2006 *IEEE Transactions on Geoscience and Remote Sensing* **44** 1259
- [32] Krotkov N, McClure B, Dickerson R, Carn S, Li C, Bhartia P, Yang K, Krueger A, Li Z, Levelt P, Chen H, Wang P and Lu D 2008 *J. Geophys. Res.* **113** D16S40
- [33] Lee C, Martin R V, van Donkelaar A, O'Byrne G, Krotkov N, Richter A, Huey L G and Holloway J S 2009 *J. Geophys. Res.* **114** D22303